JOURNAL OF SOLID STATE CHEMISTRY 116, 290–295 (1995)

# Structural Characterization and Electrical Properties of a Novel Defect Pyrochlore

J. Isasi,* M. L. López,* M. L. Veiga,* E. Ruiz-Hitzky,† and C. Pico*,[1]

*Departamento de Química Inorgánica I, Facultad de Ciencias Químicas, Universidad Complutense, 28040-Madrid, Spain; and †Instituto de Materiales, C.S.I.C. Madrid, Spain

Received June 13, 1994; in revised form October 24, 1994; accepted October 25, 1994

**Improved structural parameters for the defect pyrochlore $K_{3/2}Cr_{1/2}Te_{3/2}O_6 \cdot 0.5H_2O$ have been determined by employing a full-profile Rietveld structure analysis of X ray powder-diffraction data. These results make it possible to establish the location of the atoms in the *Fd3m* space group as follows: K (32e), Te/Cr (16d), and O (48f); the unit cell parameter is $a = 10.039$ (1). The ionic conductivity of this material has been determined by ac methods (complex impedance measurements) in pressed pellets and the obtained data suggest the unique contribution of K mobile cation, with an activation energy of 0.7 eV.** © 1995 Academic Press, Inc.

## INTRODUCTION

Ionic conductors have been extensively studied due to their potential applications as solid electrolites. Among them, mixed oxides with pyrochlore structure have received great attention because of the presence in their structure of many nonoccupied positions, which make them reasonable candidates as fast ionic conductors (1).

The cubic pyrochlore structure can be described from the ideal composition $A_2B_2X_6X'$, with eight formula units per unit cell. It is formally derived from the fluorite structure, assuming an anion vacancy in each formula. On the other hand, defect pyrochlore structure possesses an additional anion vacancy ($X'$) and it consists of a rigid framework $B_2X_6$ of vertex-sharing $BX_6$ octahedral units, in such a way that form 3D-connected tunnels which contain the $A$ cations (and the $X'$ anions in the ideal pyrochlore). These $A$ atoms are occupying half of the 32e structural sites, in the cubic space group *Fd3m* (No. 227). Therefore, the mobility of $A$ ions through the tunnels is possible. Furthermore the orientation of the tunnels is parallel to the three-fold symmetry axes, which connect the 8a and 16c sites adjacent to the 32e ones (2, 3). Other deficient pyrochlores with stoichiometric $AB_2X_6$ are also known and differ only in the occupancy degree of the 32e sites by $A$ cations. Such stoichiometry seems to be favorable for ion mobility (4).

The present work reports the structure and ionic conductivity of the defect pyrochlore oxide $K_{3/2}Cr_{1/2}Te_{3/2}O_6$, for which $K$ ($=A$) cations occupy 3/8 of the 32e sites and Cr and Te ($=B$) cations are randomly located in the 16d ones.

Previously, Danihelka (5) had reported the synthesis and characterization of the crystalline phase $K_3CrTe_3O_{12}$ (ASTM, N°37-144). He assigned a tetragonal symmetry, whose cell parameters were $a = 7102$ and $c = 11{,}594$ Å. Some conclusions obtained by this author, mainly the proposed symmetry, seem not to be correct in accordance with the reflections obtained by X ray diffraction.

## EXPERIMENTAL

The $K_{3/2}Cr_{1/2}Te_{3/2}O_6$ mixed oxide has been obtained from a stoichiometric mixture, of $Cr_2O_3$, $Te(OH)_6$, and $KNO_3$, heated at 698 K in air for 48 hr. The final compound is a green powder. X ray diffraction data show that the product was a single phase. The results of chemical analyses (ICP-AES), given in Table 1, show good agreement between calculated and observed values. The small differences are due to the fact that the compound is hydrated with 0.5 water molecules. By taking this into account, the calculated values are 15.4, 6.8, and 50.2 for K, Cr and Te, respectively.

Thermogravimetric analysis was carried out in a Mettler TG-50 thermobalance and in a DSC cell attached to a Mettler TA 3000 controller. Sample weights were about 20 mg and thermal runs were performed in $N_2$ gas flow at rate of 5 K $min^{-1}$.

Powder X ray diffraction patterns were registered at a rate of 0.1° ($2\theta$) $min^{-1}$ using a Siemens Kristalloflex diffractometer powered by a D 500 generator using Ni-filtered Cu$K\alpha$. A step scan 10°–20° ($2\theta$) and a counting time of 12 sec for each step were employed to obtain the X ray diffraction data used in the refinement of $K_{3/2}Cr_{1/2}Te_{3/2}O_6$ $0.5H_2O$. Powder X ray diffraction pat-

[1] To whom correspondence should be addressed.



0022-4596/95 $6.00

TABLE 1
Chemical Analysis of the Phase
$K_{3/2}Cr_{1/2}Te_{3/2}O_6$

| Element | % calculated | % found |
|---|---|---|
| K | 15.8 | 15.3 |
| Cr | 7.0 | 6.8 |
| Te | 51.4 | 50.2 |

terns at higher temperatures were recorded at a rate of 0.04° (2$\theta$) $min^{-1}$ using the HTK high temperature camera, mounted on a D-5000 Siemens Kristalloflex diffractometer. The experiment was carried out in vacuum.

Electrical conductivity of pressed pellets was measured in the temperature range between room temperature and 673 K in a $N_2$ gas flow. The pelletized samples were sintered at 698 K for 48 hr. Blocking electrodes were deposited on both sides of the pellets by silver paint. The conductivity was obtained by ac impedance measurements with a frequency response analyzer (Solartron 1174), attached to an electrochemical interface (Solartron 1286) over a frequency range of 1Hz–100 kHz. Resistance values were derived by interpretation of the complex impedance plane diagram of the data.

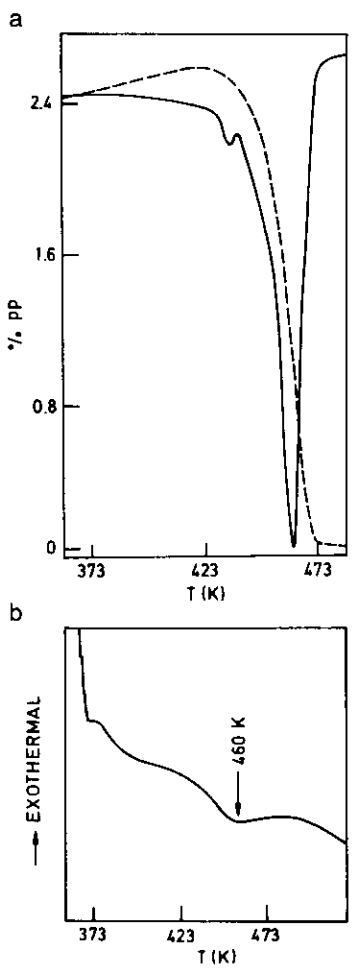


FIG. 1. TG (a) and DSC (b) experimental curves of $K_{3/2}Cr_{1/2}Te_{3/2}O_6 \cdot 0.5H_2O$.

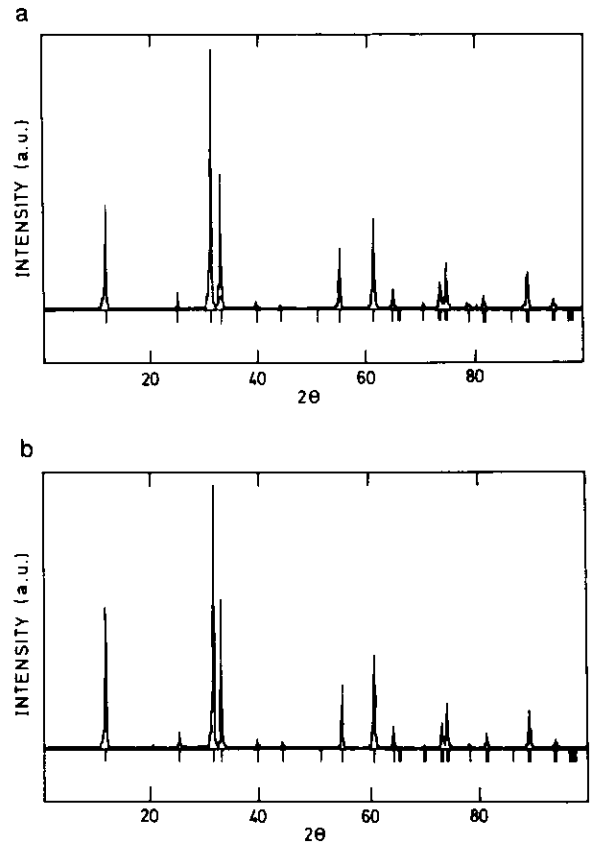


FIG. 2. XRD diagrams of oxide mixed (a) at room temperature and (b) at 700 K.

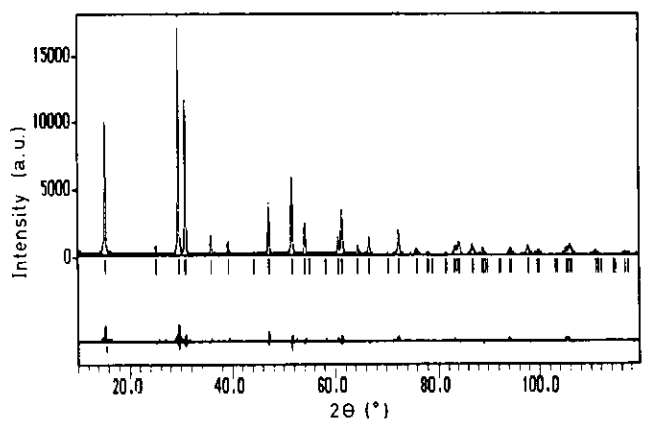


FIG. 3. The observed (· · ·) and calculated (—) and differences profiles for $K_{3/2}Cr_{1/2}Te_{3/2}O_6 \cdot 0.5H_2O$.

TABLE 2
Crystallographic Data for $K_{3/2}Cr_{1/2}Te_{3/2}O_6 \cdot 0.5H_2O$[a]

| | | | |
|---|---|---|---|
| K | 32e | $(x, x, x)$ $x = 0.108(1)$ | Occ = 3/8 |
| O($H_2O$) | 32e | $(x, x, x)$ $x = 0.108(1)$ | Occ = 1/8 |
| Te, Cr | 16d | 1/2, 1/2, 1/2 | Occ = 1 |
| O | 48f | u, 1/8, 1/8 $u = 0.421(4)$ | Occ = 1 |

[a] Cubic, $Fd3m$, $a = 10.033$, $R_p = 16.7$, $R_{wp} = 16.5$, $R_B = 4.8$, $\chi^2 = 2.0$.

TABLE 3
Bond distances (in Å) for $K_{3/2}Cr_{1/2}Te_{3/2}O_6 \cdot 0.5H_2O$

| | | | |
|---|---|---|---|
| $K-O_i$ | 3.153(1) × 3 | Cr/Te–O | 1.941(2) × 6 |
| $K-O_{ii}$ | 3.368(1) × 3 | Shannon | 1.98 |
| $K-O_{iii}$ | 2.810(1) × 3 | | |
| Mean | 3.11 | | |
| Shannon | 2.93 | | |

## RESULTS AND DISCUSSION

Figure 1 shows TG and DSC curves for this compound. A weight loss corresponding to half a water molecule are deduced from the TG curves. Such weight loss is observed toward 460 K. In the DSC graph an endotermic effect is observed around this temperature. Similar results have been obtained for other related pyrochlore such as $KWTaO_6 \cdot H_2O$ (7, 8).

We have carried out X ray diffraction studies at different temperatures (in the range from 300 to 700 K) in order to characterize the corresponding dehydrated compound. The X ray diffraction pattern obtained at 623 K, Fig. 2, shows light variations in the intensity and in the $2\theta$ value for the reflections. These results are compatible with a slight decrease in the cell parameter for $K_{3/2}Cr_{1/2}Te_{3/2}O_6$ when $a = 10.021(3)$ Å.

For $K_{3/2}Cr_{1/2}Te_{3/2}O_6 0.5H_2O$ the X ray diffraction data indicate that this mixed oxide has the characteristic reflections of a defect pyrochlore structure. Rietveld's profile analysis method (4) was applied for refinement of this compound using X ray diffraction data. A pseudo-Voight function was chosen to generate the line shape of the diffraction peaks. Refinement was carried out in the cubic space group $Fd3m$ (No. 227). The best discrepancy factors for the Rietveld's refinement were obtained with the oxygen atoms in 48f, the Cr and Te atoms randomly distributed in 16d and the K ion and the water molecule occupying 3/8 and 1/8 of the 32e positions, respectively. The agreement between the observed and calculated profiles is shown in Fig. 3. The refined structural parameters are listed in Table 2. The most representative bond lengths and angles for these materials are given in Table 3. The observed interatomic distances are comparable to the sums of the radii of Shannon (9). Cr and Te are centered in their respective octahedra with six equal bond distances and K atoms are surrounded by 3 + 3 + 3 anions, Fig. 4a.

In Fig. 4b the structural model for this compound is shown. Corner-sharing $(Cr/Te)O_6$ octahedra form a rigid network, $B_2O_6$, in such a way that intersecting tunnels in three dimensions are created in this structure. The K atoms are located in these tunnels (10).

As well as other mixed oxides with pyrochlore structure (11–13), the $K_{3/2}Cr_{1/2}Te_{3/2}O_6$ compound can behave as a good solid electrolite due to "delocalization" of the $K^+$ ions in the 8a, 16c, and 32e positions (11). Furthermore, the tunnel's great size in this structure allows the defect pyrochlores to possess high $A^+$ cation mobility and hence exhibit good ionic conductivity.

Electrical conductivity for $K_{3/2}Cr_{1/2}Te_{3/2}O_6$ materials have been determined by ac methods. In order to under-

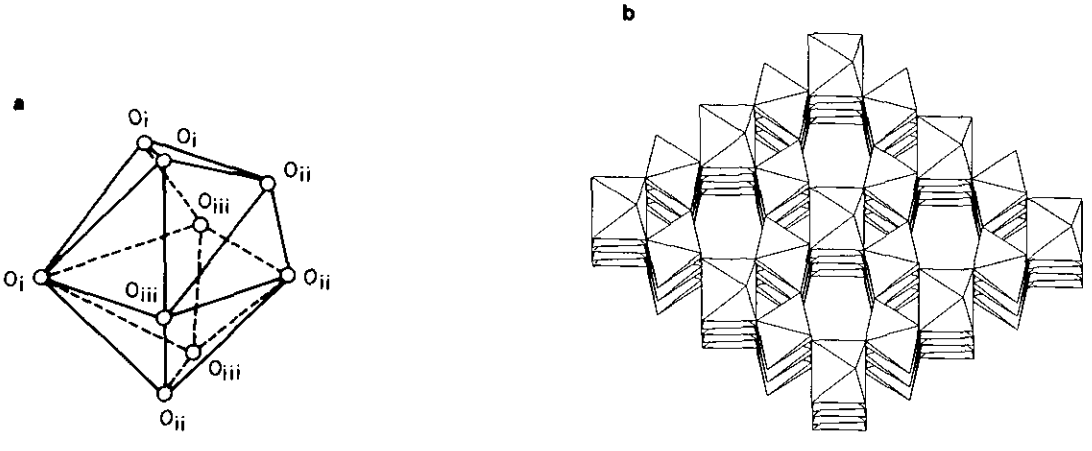


FIG. 4. (a) Coordination polyhedra of K atom. (b) Rigid network of $BO_6$ octahedra in pyrochlore structure.

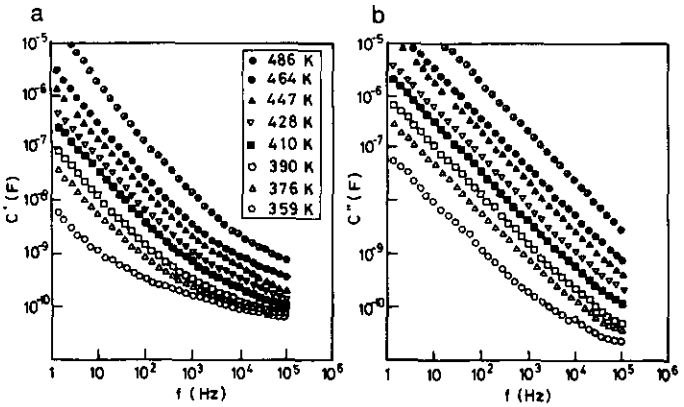


FIG. 5. (a) $C'$ and (b) $C''$ vs frequency at different temperatures for $K_{3/2}Cr_{1/2}Te_{3/2}O_6 \cdot 0.5H_2O$.

stand better the electrical nature of solid electrolites, ac conductivity analysis was used by many researchers (16–19) including the complex impedance and modulus spectroscopy. These techniques are useful in eliminating polarization and grain boundaries effects (19) when evaluating the true dc conductivity.

Real and imaginary parts of the capacitance are depicted in Figs. 5a and 5b as a function of the frequency for this mixed oxide at various temperatures. The real part of capacitance is proportional to $w^{-(1-n)}$, for low frequency values (14). This behavior is characteristic of interactions between mobile cations occupying neighboring sites in the tunnels along which the conduction takes place. The $C''$ response is dominated by a true dc conduction mechanism as deduced from the $-1$ slope in the $C''$ graph (Fig. 5b).

Typical plots of ac conductivity data are shown in Fig. 6 over a wide range of temperatures. All curves in this figure show a frequency-independent plateau corresponding to dc conductivity effects. At higher frequencies the conductivity dispersion follows the power-law dependence as observed in many hopping ion-conductors (15). The experimental points were fitted to a single power law as follows: $\sigma(w) = \sigma(o) + Aw^n$, where $\sigma(o)$ is a dc term associated to the mobile charge, $A$ is a temperature-dependent parameter, and $n$ is the slope of high frequency dispersion data ($n$ assumes a value between 0 and 1).

Modulus ($M''$) and impedance ($Z''$) spectra vs log frequency are given in Fig. 7 for $K_{3/2}Cr_{1/2}Te_{3/2}O_6$ at 376 K.

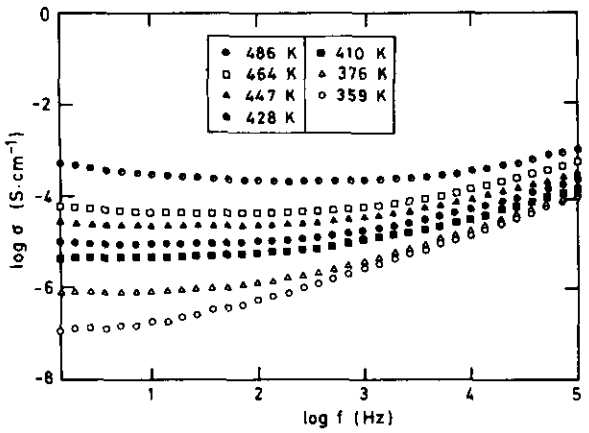


FIG. 6. Plots of log of conductivity vs log of frequency at different temperatures.

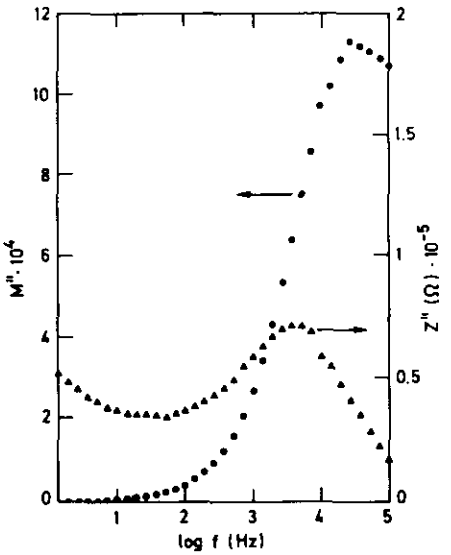


FIG. 7. Impedance and modulus spectra at 373 K.

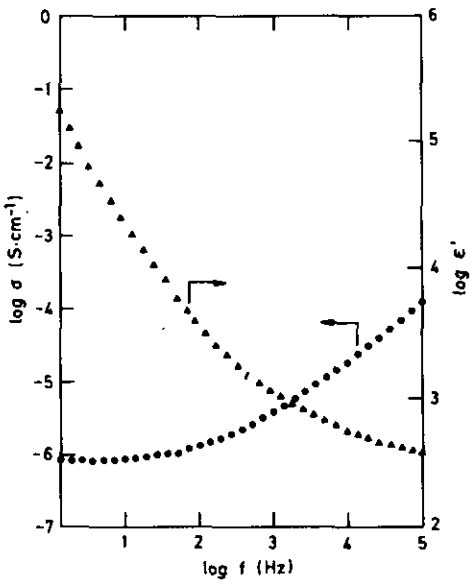


FIG. 8. Conductivity and permittivity vs log of frequency at 373 K.

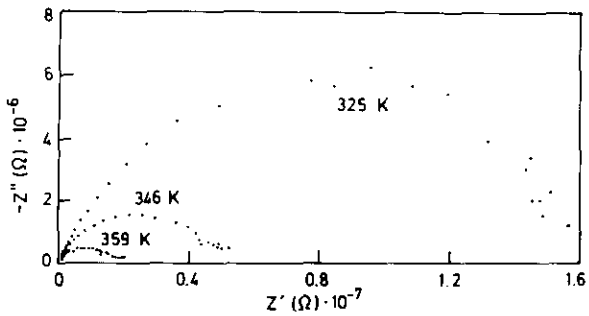


FIG. 9. Complex impedance plots at various temperature for $K_{3/2}Cr_{1/2}Te_{3/2}O_6 \cdot 0.5H_2O$.

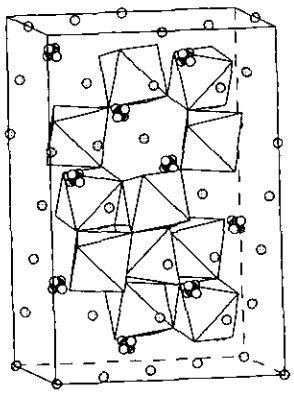

FIG. 11. Structure of $K_{3/2}Cr_{1/2}Te_{3/2}O_6 \cdot 0.5H_2O$, Octahedra Cr/Te: white circles, 32e positions; dots circles, 16c positions; and shadow circles, 8a positions.

Such a graph shows that this polycrystalline material is not an ideal electrolyte since the peaks in the $M''$ and $Z''$ spectra are broader than Debye peaks, and the frequencies of the peak maxima in the two spectra do not coincide.

The broad peak in the modulus spectrum can be assigned to summation of relaxations occurring within the bulk material (as opposed to interfacial or intergranular effects). Moreover, the high-frequency dispersion in $\sigma$ starts at a frequency corresponding to the maximum in $Z''$ and most of the related dispersion in $\varepsilon'$ (Fig. 8) was completed at a frequency corresponding to the maximum in $M''$. For an ideal electrolyte these frequencies would coincide and there would be dispersion, but for real electrolytes the maxima in $M''$ and $Z''$ span a range of frequencies. When intergranular effects are present, this frequency range is more extended (19).

For an ideal electrolyte, the peak height is $1/3\varepsilon'$. From Fig. 8 we can assume a permittivity value of 400, and therefore the theoretical height for a single Debye peak is 1/800 (ca. 1.2E-3). This value is in good agreement with the experimental value, $M'' = 1.1E\text{-}3$. Also, for an ideal electrolyte, the peak positions are given by $f_{max} = \sigma/2\pi e_o\varepsilon'$. If $\varepsilon' = 400$ and $\sigma = \sigma_0$ (the plateau of $\sigma$, Fig. 8), $\log f_{max} = 3.65$, again in good agreement with the experimental value 3.5. This criterion can only be satisfied if grain boundary effects are absent.

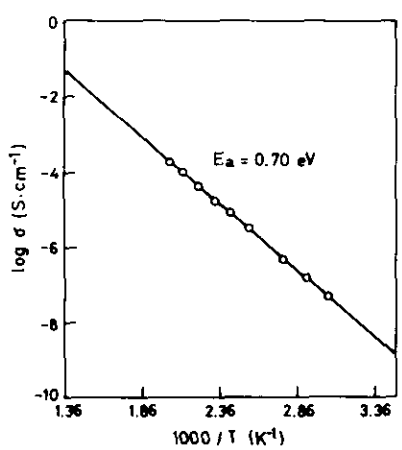


FIG. 10. Arrhenius plots of $K_{3/2}Cr_{1/2}Te_{3/2}O_6 \cdot 0.5H_2O$.

Complex plane plots at three different temperatures are presented in Fig. 9, showing the tilted semicircular arcs characteristic of ionic conductors. dc conductivity is obtained from extrapolation of the semicircular arcs with the real axis or from frequency-independent plateau ($\sigma_O$) in ac conductivity vs $\log f$ plots. Both methods lead to the same results. The temperature dependence of the ionic conductivity is presented in Fig. 10. This Arrhenius plot yielded a straight line from whose slope the energy for ion motion has been deduced. The activation energy for $K_{3/2}Cr_{1/2}Te_{3/2}O_6$ has been obtained giving a value of 0.7 eV. This value is similar to the data achieved in other potassium materials with defect pyrochlore structure (12).

This activation energy is indicative that the mixed oxide is a good ionic conductor. We think the ionic conductivity is due to correlated motion of the $K^+$ ions as in other pyrochlore compounds (12). The $K^+$ are occupying 32e positions located along the channels in the rigid network of the $BO_6$ octahedra. Figure 11 shows a representation of these channels. A hexagonal planes ring lies on a diagonal plane of the cube, normal to the 8a–16c–8a axis. Tetrahedra are formed by the 32e positions around 8a, being occupied in only three out of every eight (1.5/4). This partial occupation enables the displacement of the $K^+$ ions along these channels.

## ACKNOWLEDGMENTS

This work has been supported by DGICYT (PB92-0124) and CICYT (MAT94-0729) for financial support. The authors thank Dr. J. C. Galván and Dr. R. Jiménez for their help with the measurements and discussion.

## REFERENCES


1. M. A. Subramanian, G. Aravamudan, and G. V. Subba Rao, *Prog. Solid State Chem.* **15,** 132 (1983).
2. S. García-Martín, A. Jerez, C. Pico, M. L. Veiga, G. González-Diaz, F. Sanchez-Quesada, and J. Santamaría, *Solid State Ionics* 455 (1992).
3. C. Michel and B. Raveau, *Mater. Res. Bull.* **8,** 451 (1973).
4. A. Jerez, M. L. López, S. García-Martín, M. L. Veiga, and C. Pico, *J. Mater. Sci.* **26,** 5163 (1991).
5. Danielka, *Collect. Czech. Chem. Commun.* **48,** 2197 (1983).
6. R. Rodríguez-Carvajal, "Fullprof" Program, ILL. Grenoble, France, 1990.
7. S. García-Martín, M. L. Veiga, M. Gaitán, A. Jerez, C. Pico, and J. Santamaría, *Solid State Ionics* **27,** 195 (1988).
8. B. Darriet, H. Rat, J. Galy, and P. Hagenmuller, *Mater. Res. Bull.* **6,** 1305 (1971).
9. R. D. Shannon, *Acta Crystallogr. Ser. A* **32,** 751 (1976).
10. R. Yvon, W. Jeitschko, and E. Parthé, *J. Appl. Crystallogr.* **10,** 73 (1977).
11. B. Raveau, *Rev. Inorg. Chem.* **1,** 8 (1979).
12. J. Grins, M. Nygren, and T. Wallin, *Mater. Res. Bull.* **15,** 53 (1980).
13. A. D. English, A. W. Sleight, J. L. Fouequet, and R. Delape, *Mater. Res. Bull.* **15,** 1727 (1980).
14. A. K. Jonscher, "Dielectric Relaxation in Solids." Chelsea Dielectric Press, London, 1983.
15. A. K. Jonscher, *Nature* **264,** 673 (1977).
16. I. D. Raistrick, *Solid State Ionics* **18/19,** 40 (1986).
17. D. P. Almond, G. K. Duncan, and A. R. West, *Solid State Ionics* **8,** 159 (1983).
18. B. V. R. Chowdari, K. Radhakrishnan, K. A. Thomas, and G. V. Subba Rao, *Mater. Res. Bull.* **24,** 221 (1989).
19. I. M. Hodge, M. D. Ingram, and A. R. West, *J. Electroanal. Chem.* **74,** 125 (1976).